Ultramicroscopy 18 (1985) 33–38
North-Holland, Amsterdam

IMAGE LOCALISATION

L.D. MARKS *

Department of Physics, Arizona State University, Tempe, Arizona 85287, USA

Received 3 June 1985; presented at Symposium January 1985

This paper briefly discusses localisation in high-resolution electron microscope images, i.e. the extent to which one can consider the images as faithful representations of the individual atomic columns. Firstly we indicate how the tightly bound nature of the Bloch waves at a zone axis automatically generates diffractive localisation. We then deal with the imaging, the main source of delocalising effects. By using a pseudo-Wannier analysis, we indicate how a localisation function can be defined and also how the different microscope aberrations can partially cancel to produce localised images.

1. Introduction

One of the main strengths of high-resolution electron microscopy, and indeed any type of electron microscopy, is microstructural analysis. One recent advance has been the demonstration that it is possible to refine the locations of *individual* atomic columns, e.g. refs. [1–4]. The fact that one can obtain such highly localised information is, with respect to some of the available analyses in the literature, somewhat surprising. Extrapolating from the known break-down of the column approximation for weak beam images (e.g. refs. [5–7]) to high-resolution images suggests that it should not be possible to obtain localisation except in very thin specimens. Similarly, a simplistic idea of the lens defocus and other aberrations as acting to blur the image would also prevent any localisation. In fact, as we will briefly discuss in this note, ideas such as image blurring and the breakdown of the column approximation are not applicable to high-resolution zone axis imaging. Firstly, we indicate how the tightly bound nature of the Bloch waves at a zone axis automatically generates diffractive localisation. We then deal with the imaging, the main source of delocalising effects. By using a pseudo-Wannier analysis, we indicate how a localisation function can be defined and also how the different microscope aberrations can partially cancel to produce localised images. The column approximation is excellent for a zone axis orientation, whilst there are cancelling effects in the imaging which minimise delocalising effects such as Fresnel oscillations.

2. Diffractive localisation

The basic reason why the diffraction is localised has been implicitly available in the literature for many years, but has not been fully spelt out. To understand the underlying physics, we need to consider the diffraction in terms of Bloch waves. These are similar to the waves that are used to describe the valence/conduction electrons in solids, except that we are interested in the very high energy levels rather than those of low energy. As with a band structure analysis, the solid potential mixes together different wavevectors; that is, it introduces diffraction effects. The strength of this coupling depends upon the depth of the potential and a relativistic interaction term. Due to relativistic effects this interaction term does not steadily decrease as the electron energy increases but instead levels off. Thus the high-energy electrons

* Present address: Department of Materials Science and Engineering, The Technological Institute, Northwestern University, Evanston, Illinois 60201, USA.

"see" a deep potential, analogous to a tightly bound insulator.

More rigorously, we can see this effect if we look for solutions for a wave of form $\psi(\mathbf{r})\exp(2\pi i z/\lambda)$, where λ is the electron wavelength. Substituting into the relativistically corrected Schrödinger equation, and neglecting the term of order λ^2 as small, we find:

$$\frac{\partial\psi(\boldsymbol{r})}{\partial z} = i\left[\left(\frac{h(1-\beta^2)^{1/2}}{2\pi v m_0}\right)\nabla_\rho^2 + \frac{4\pi c^2}{hv}V(r)\right]\psi(\boldsymbol{r}), \tag{1}$$

where

$$\nabla_\rho^2 = \partial^2/\partial x^2 + \partial^2/\partial y^2.$$

As the voltage increases, i.e. the electron velocity v increases, the term

$$h(1-\beta^2)^{1/2}/2\pi v m_0$$

which governs the strength of the transverse spreading drops faster than the term $4\pi c^2/hv$ which parametrizes the strength of the interaction with the specimen potential. The ratio of the two, essentially the localisation of the scattering, increases noticeably with the electron velocity.

What this means for the Bloch waves is that the dispersion surface is comparatively flat. The dispersion surface is a geometrical construction for the allowed values $\boldsymbol{k}_j$ of the Bloch waves:

$$B_j(\boldsymbol{r}, \boldsymbol{k}_j) = \sum_g C_g^j(\boldsymbol{k}_j)\exp\left[2\pi i(\boldsymbol{k}_j + \boldsymbol{g})\cdot\boldsymbol{r}\right], \tag{2}$$

where the total wavefunction is:

$$\psi(\boldsymbol{r}) = \exp\left(\frac{-2\pi i z}{\lambda}\right)\sum_j C_0^j(\boldsymbol{k}_j)B_j(\boldsymbol{r}, \boldsymbol{k}_j). \tag{3}$$

In optics, the dispersion surface (surface of constant phase) governs the propagation of a wave; the vector normal to the surface determines the propagation direction of the wave, whilst the curvature of the surface determines the transverse (normal to the incident direction) spreading. On a zone axis all the propagation directions are parallel to the incident direction as illustrated in fig. 1 and, due to the flatenss of the surfaces (tightly bound nature), the transverse spreading is small.

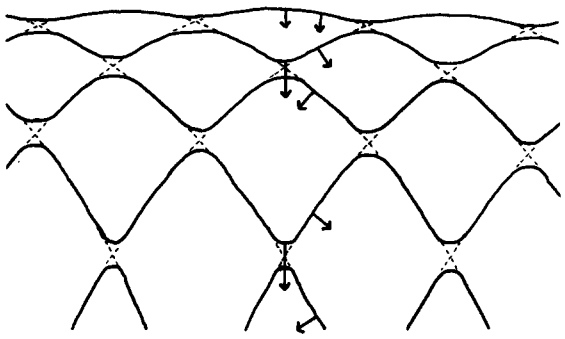

Fig. 1. Schematic dispersion surface. On the zone axis the surfaces are relatively flat and perpendicular to the incident beam direction. Thus the Bloch waves all propagate down the zone axis and the second-order transverse spreading due to the curvature of the surfaces is small.

This is completely different from a weak beam orientation when the Bloch waves propagate in different directions, leading to the breakdown of the column approximation. Due to the tightly bound nature of the scattering, to an excellent approximation the final wave can be represented by the phase grating form. This approximation improves as we use higher voltages and heavier elements (deeper potentials). Note that the angular spread of the illumination within the crystal will not seriously affect the approximation; variations in the diffraction conditions turn out to be minimised by cancelling effects in the imaging [8]. However, in thicker crystals phonon scattering will increase the occupancy of the more weakly bound states leading to increased delocalisation of the information.

3. Lens localisation

Given that we may consider the diffraction in terms of independent columns of atoms, we now have to consider the effects of the microscope imaging system. As a rule it is the imaging that will defeat procuring a localised image.

One problem with understanding the criteria for localisation is that simplistic contrast transfer function analyses in reciprocal space can be misleading. The information concerning position is contained in the relative phases of different beams.

A spatially variant phase shift arising from the C_s and defocus will extend the signal from any one column of atoms, in principle leading to Fresnel-like fringes of infinite extent. The other microscope aberrations (such as focal spread and convergence) come in as terms which limit the width of the Fresnel-like oscillation. The phase-shift term can be thought of as leading to a complex Gaussian spread function in the image, the envelope as leading to a real Gaussian [2,9]. The appropriate balance between the two eliminates the long-range oscillations, thus increasing the localisation of the images [2].

We may readily make the above discussion more quantitative. We consider each diffracted component of the exit wave as spatially varying via a shape function, i.e.

$$\psi(\boldsymbol{r}) = \sum_{\boldsymbol{g}} \exp(2\pi i \boldsymbol{g}\cdot\boldsymbol{r})\ \varphi_{\boldsymbol{g}}(\boldsymbol{r})$$

$$= \sum_{\boldsymbol{g}} \exp(2\pi i \boldsymbol{g}\cdot\boldsymbol{r}) \int \Phi_{\boldsymbol{g}}(\boldsymbol{u}) \times \exp(-2\pi i \boldsymbol{u}\cdot\boldsymbol{r})\ \mathrm{d}^2\boldsymbol{u}, \quad (4)$$

where this integral and also those in eqs. (6) and (8) below are over the reciprocal unit cell. (All the variables in eq. (4) and the rest of this section are implicitly in the plane normal to the incident beam.) We now use what is essentially a Wannier-type of analysis, see for instance refs. [10,11], and rewrite eq. (4) using the substitution:

$$\varphi_{\boldsymbol{g}}(\boldsymbol{r}) = N^{-1/2} \sum_{\boldsymbol{r}_n} \varphi_{\boldsymbol{g}}(\boldsymbol{r}_n)\ \omega(\boldsymbol{r}-\boldsymbol{r}_n), \quad (5)$$

where

$$w(\boldsymbol{r}-\boldsymbol{r}_n) = N^{-1/2} \int \exp(-2\pi i \boldsymbol{u}\cdot[\boldsymbol{r}-\boldsymbol{r}_n])\ \mathrm{d}^2\boldsymbol{u}, \quad (6)$$

with N the number of lattice points $\boldsymbol{r}_n$. We have in eq. (5) a spatial modulation $\varphi(\boldsymbol{r}_n)$ of a wave term in the image plane $w(\boldsymbol{r}-\boldsymbol{r}_n)$. Within the weak phase object approximation, we may write for the image intensity $I(\boldsymbol{r})$

$$I(\boldsymbol{r}) = 1 - 2N^{-1/2} \sum_{\boldsymbol{g}} \cos(2\pi \boldsymbol{g}\cdot\boldsymbol{r}) \sum_{\boldsymbol{r}_n} w(\boldsymbol{r}-\boldsymbol{r}_n) \times \left(\varphi_{\boldsymbol{g}}(\boldsymbol{r}_n) \square L(\boldsymbol{r}_n)\right), \quad (7)$$

where the convolution, $\square$, is over lattice points $\boldsymbol{r}_n$ and

$$L(\boldsymbol{r}_n) = N^{-1/2} \int [T(\boldsymbol{g}+\boldsymbol{u}) + T^*(-\boldsymbol{g}-\boldsymbol{u})] \times \exp(-2\pi i \boldsymbol{u}\cdot\boldsymbol{r}_n)\ \mathrm{d}^2\boldsymbol{u}, \quad (8)$$

$T(\boldsymbol{u})$ being the standard linear contrast transfer function. (One can use a semi-linear form, see ref. [9], without any complications to generate a more accurate result.) $L(\boldsymbol{r}_n)$, which we will refer to as the localisation function, has a simple physical interpretation. It only exists at the lattice points, $\boldsymbol{r}_n$, and indicates to what extent the information at any one lattice point also contributes to other lattice points. Thus $L(\boldsymbol{r})$ will only be significant at the origin for a localised image, and large everywhere for a delocalised image. A localised image will occur if $T(\boldsymbol{u})$ is only slowly varying around the $\boldsymbol{g}$ beam, not simply if the transfer function is large for the $\boldsymbol{g}$ beam. $L(\boldsymbol{r}_n)$ is also simple to calculate because of the inbuilt consistency test that the average value is the CTF value for the $\boldsymbol{g}$ beam. Numerical values for the localisation function for crossed gold (111) fringes for the Cambridge High-Voltage High-Resolution Electron Microscope are shown in fig. 2 for three different defoci and three different values for the focal spread. The "dots" in the images represent the lattice points, white indicating a positive transfer at that point, black negative. Thus for the -200 Å defocus images the information in any one atomic column is present not only in the image of this column, but also in the neighbouring columns. In contrast, for -600 Å defocus the information is localised to the atomic column where it originates. Note that a large increase *or* decrease in the energy spread would tend to delocalise the images; by chance the Cambridge microscope is nearly ideal for imaging gold. The loss of image localisation for the defocus of -200 Å is apparent in the experimental results (see particularly fig. 3 in ref. [2]; a surface dislocation which is apparent in images taken at -600 Å defocus is averaged out and thus invisible at -200 Å defocus).

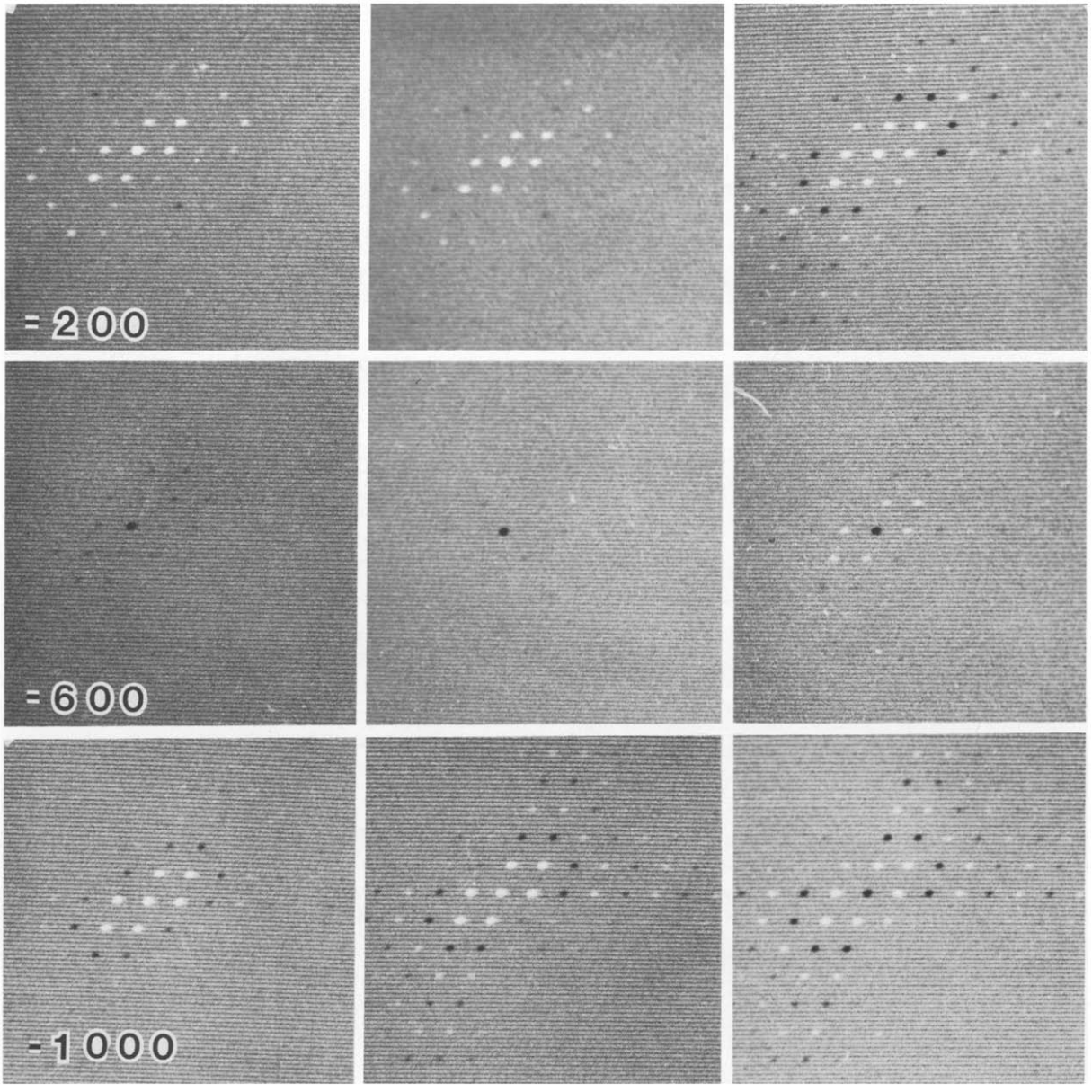

Fig. 2. Localisation function for the Cambridge HREM for three defoci as marked on the left. Across the page the defocus spread is 80, 160 and 320 Å respectively. Note that the optimum localisation is for 160 Å of defocus spread.

4. Discussion

We have discussed here, briefly, the main factors which determine the localisation in high-resolution images. On a zone axis it is fairly safe to employ an atomic column approximation, particularly at high voltages and for heavy elements due to the tightly bound nature of the Bloch waves. A balance between the different aberrations can lead to image localisation, quite strongly dependent upon the precise operating conditions of the instrument. Since a shift of $\boldsymbol{d}$ in the location of an

atomic column leads to a phase shift of $2\pi i \boldsymbol{d} \cdot \boldsymbol{u}$, and thus alters the phases of the low-order beams, we can aim for quite accurate determination of the locations of individual atomic columns. Note that the analysis herein is based upon the use of a coherent electron wavepacket, and as such holds not only for a perfect crystal, but *also* around any crystal defects or surfaces. As discussed elsewhere [2], the main limitation is the ratio of the signal strength to the shot-noise, not some arbitrary Scherzer information limit.

5. Conclusions

The diffraction from heavy elements at high voltages on a zone axis is inherently localised in the image plane. The imaging system is the prime source of delocalisation, but there are cancelling effects. This can be simply described using a pseudo-Wannier analysis by a localisation function.

Acknowledgements

This work was supported on Department of Energy Grant No. DE-AC02-76ER02995.

References

[1] L.D. Marks, Phys. Rev. Letters 51 (1983) 1000.
[2] L.D. Marks, Surface Sci. 139 (1984) 281.
[3] A. Bourret, C. Anterroches and J.M. Pennsson, J. Physique 43 (1982) 83.
[4] A. Crecy and A. Bourret, Phil Mag. A47 (1983) 245.
[5] A. Howie and Z.S. Basinski, Phil Mag. 17 (1968) 1039.
[6] A. Howie and C.H. Sworn, Phil Mag. 22 (1970) 861.
[7] C.J. Humphreys, Rept. Progr. Phys. 42 (1979) 122.
[8] L.D. Marks, Ultramicroscopy 14 (1984) 351.
[9] L.D. Marks, Ultramicroscopy 12 (1983–84)) 237.
[10] J.M. Ziman, Principles of the Theory of Solids (Cambridge University Press, Cambridge, 1972).
[11] C. Kittel, Quantum Theory of Solids (Wiley, New York, 1963).